In situ induction of dendritic cell–based T cell tolerance in humanized mice and nonhuman primates

Kyeong Cheon Jung,[1,2] Chung-Gyu Park,[3,4,8] Yoon Kyung Jeon,[1] Hyo Jin Park,[1] Young Larn Ban,[2] Hye Sook Min,[1] Eun Ji Kim,[2] Ju Hyun Kim,[1] Byung Hyun Kang,[2] Seung Pyo Park,[7] Youngmee Bae,[5] Il-Hee Yoon,[3,4,8] Yong-Hee Kim,[3,4,8] Jae-Il Lee,[8] Jung-Sik Kim,[3,4,8] Jun-Seop Shin,[3,4,8] Jaeseok Yang,[6,9] Sung Joo Kim,[10,11] Emily Rostlund,[12] William A. Muller,[12] and Seong Hoe Park[1,2]

[1]Department of Pathology, [2]Graduate School of Immunology, [3]Department of Microbiology and Immunology, [4]Cancer Research Institute, [5]Department of Parasitology and Tropical Medicine, and [6]Transplantation Research Institute, College of Medicine; and [7]National Creative Research Initiative Center for Oxide Nanocrystalline Materials, School of Chemical and Biological Engineering, College of Engineering; Seoul National University, Seoul 151-742, South Korea
[8]Xenotransplantation Research Center and [9]Transplantation Center, Seoul National University Hospital, Seoul 110-744, South Korea
[10]Department of Surgery and [11]Department of Molecular Medicine, Samsung Medical Center, Sungkyunkwan University School of Medicine, Seoul 135-710, South Korea
[12]Department of Pathology, Northwestern University Feinberg School of Medicine, Chicago, IL 60611

Induction of antigen-specific T cell tolerance would aid treatment of diverse immunological disorders and help prevent allograft rejection and graft versus host disease. In this study, we establish a method of inducing antigen-specific T cell tolerance in situ in diabetic humanized mice and Rhesus monkeys receiving porcine islet xenografts. Antigen-specific T cell tolerance is induced by administration of an antibody ligating a particular epitope on ICAM-1 (intercellular adhesion molecule 1). Antibody-mediated ligation of ICAM-1 on dendritic cells (DCs) led to the arrest of DCs in a semimature stage in vitro and in vivo. Ablation of DCs from mice completely abrogated anti–ICAM-1–induced antigen-specific T cell tolerance. T cell responses to unrelated antigens remained unaffected. In situ induction of DC-mediated T cell tolerance using this method may represent a potent therapeutic tool for preventing graft rejection.

CORRESPONDENCE
Seong Hoe Park:
pshoe@snu.ac.kr

Abbreviations used: Gal, galactose-α-1,3-galactose; HSC, hematopoietic stem cell; HUVEC, human umbilical vein endothelial cell; IEQ, islet equivalent; IT, immunotoxin; MLR, mixed lymphocyte reaction; STZ, streptozotocin.

Tolerance to specific antigens is the ultimate therapeutic goal in two major immunological fields, autoimmunity and transplantation rejection. Over the past several decades, the generation of a large array of immunosuppressive agents has increased the number of therapeutic tools available to address these two issues. The focus has now shifted to tackling the side effects of long-term immunosuppression. The final goal is to achieve T and B cell tolerance that is antigen specific without the need for long-term generalized immunosuppression.

The mechanisms that underlie peripheral T cell tolerance have been explained, in part, although some points remain to be addressed. DCs have a key role in immune regulation (Steinman et al., 2003). Antigen presentation by immature and semimature DCs results in immune tolerance rather than effective T cell immunity because of the failure to provide sufficient co-stimulatory signals (Reis e Sousa, 2006; Morelli and Thomson, 2007; Shortman and Naik, 2007). These tolerogenic DCs are characterized by low-level expression of surface MHC molecules and several other co-stimulatory receptors and the production of low levels of Th1 cytokines, notably IL-12p70 (Morelli and Thomson, 2007).

Among several mouse anti–human ICAM-1 (intercellular adhesion molecule 1) antibody clones we have developed thus far, we were able to select only one clone, MD-3, which

K.C. Jung and C.-G. Park contributed equally to this paper.

The Rockefeller University Press $30.00
J. Exp. Med. Vol. 208 No. 12 2477-2488
www.jem.org/cgi/doi/10.1084/jem.20111242

The Journal of Experimental Medicine

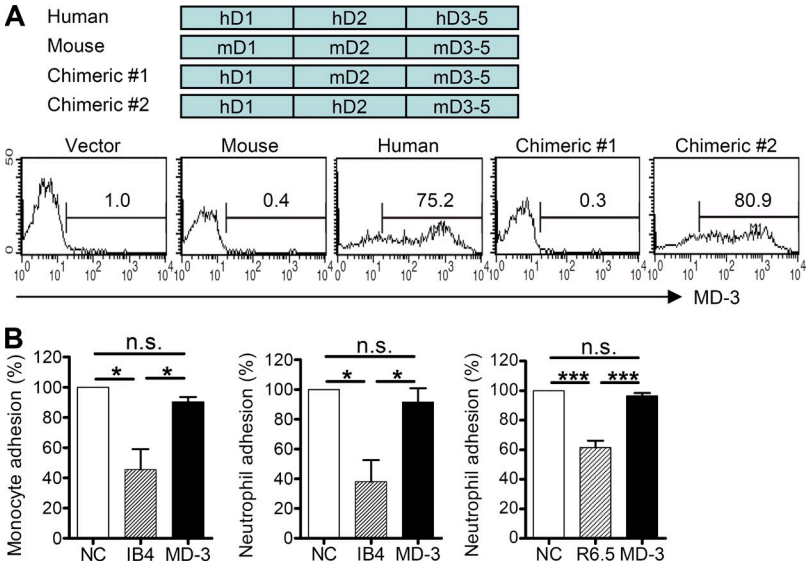

Figure 1. Development of an anti–human ICAM-1 antibody. (A) HEK293 cells were transfected with vector alone or vector encoding domains 1, 2, or 3–5 of human (h) or mouse (m) ICAM-1. MD-3 binding was assessed by flow cytometry. (B) PBMCs or neutrophils were incubated with human umbilical vein endothelial monolayers in the absence (negative control [NC]) or presence of monoclonal antibodies specific for CD18 (IB4) or ICAM-1 (R6.5) with MD-3, all at 20 µg/ml. Adhesion was measured as described in Materials and methods. Data are expressed as the mean adhesion relative to control ± SE of three experiments (except IB4 in the monocyte adhesion assay, where $n = 2$), with six replicates per experiment. n.s., not significant; *, $P < 0.05$; ***, $P < 0.001$.

was cross-functional with ICAM-1 molecules on nonhuman primates. Epitope-based ligation of ICAM-1 on immature DCs with this antibody led to the arrest of DCs in a semi-mature stage. They expressed low levels of MHC and co-stimulatory molecules on their surfaces and displayed significantly lower production of inflammatory cytokines.

The generation of humanized mice through the engraftment of human hematopoietic stem cells (HSCs) provides a powerful tool for investigating various human biological processes, notably in vivo immune responses, the study of which would otherwise not be possible (Ito et al., 2002; Manz, 2007; Shultz et al., 2007; Brehm et al., 2010; Issa et al., 2010). Engraftment of human HSCs in NOD.SCID/$\gamma c^{-/-}$ (NOG) mice is more efficient than other previously described humanized mouse models (Ito et al., 2002; Brehm et al., 2010). These mice exhibit long-term engraftment of HSCs in the recipient bone marrow and generation of all human blood lineage cells in the periphery (Hiramatsu et al., 2003; Traggiai et al., 2004). Current humanized mouse models have some minor defects, particularly in innate immunity, such as incomplete reconstitution of NK cells and poor development of myeloid lineage cells (Chen et al., 2009). However, unlike the hu-PBL-SCID mouse, which lacks normal lymphoid organs and architecture (Tary-Lehmann et al., 1995), the immune cells in the spleens of NOG mice reconstituted with human HSCs showed a fairly good organization into white and red pulp (Strowig et al., 2009). In particular, the model allows effective reconstitution of T and B cells. Moreover, T cells in these humanized mice were able to control infection with Epstein-Barr virus (Strowig et al., 2009). In this respect, a humanized mouse can be considered to be the most appropriate animal model for the assessment of the human immune system (Shultz et al., 2007).

We previously provided theoretical evidence for the generation of a unique population of $CD4^+$ T cells, so-called T-T $CD4^+$ T cells, that are restricted by human MHC class II molecules on thymocytes rather than by those on mouse thymic epithelial cells in humanized mice (Choi et al., 1997, 2005; Lee et al., 2010). These T cells have a diverse TCR repertoire (Choi et al., 2005; Li et al., 2005). Moreover, a recent study from our laboratory demonstrated that T-T $CD4^+$ T cells do exist in humans (Lee et al., 2010; Min et al., 2011). Most recently, PLZF (promyelocytic

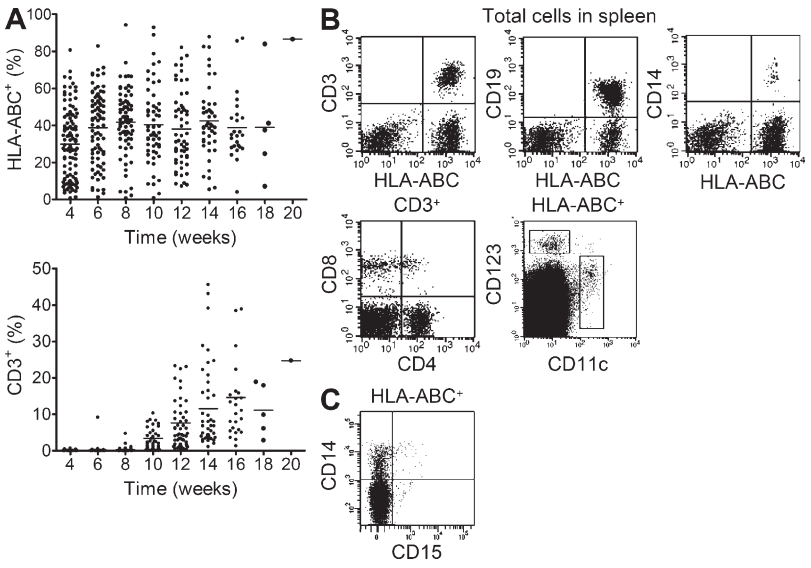

Figure 2. Human hematopoietic cell engraftment and immune cell development in humanized mice. (A) Data represent the percentage of human HLA-ABC^+ or $CD3^+$ cells in the peripheral blood of consecutively analyzed mice at the indicated weeks after transplantation of human $CD34^+$ cells. Cumulative data ($n = 111$) were obtained from >10 independent experiments. Horizontal bars indicate the mean. (B) Flow cytometry data show $CD4^+CD3^+$ or $CD8^+CD3^+$ T cells, B cells ($CD19^+$), monocytes ($CD14^+$), and conventional ($CD11c^+$) or plasmacytoid ($CD123^+$) DCs in the spleen. Data shown are representative of more than five independent experiments. (C) Flow cytometry data show the individual population of $CD14^+CD15^-$ monocytes and $CD14^-CD15^+$ neutrophils in the peripheral blood. Shown are representative data from one experiment of two mice.

leukemia zinc finger)-negative T-T CD4+ T cells were shown to be similar to conventional naive T cells with respect to a lack of expression of activation/memory markers and to be functionally equivalent to conventional naive CD4+ T cells in terms of B cell help (Kim et al., 2011). Therefore, humanized mice can be considered to be representative models that mimic the human immune system (Issa et al., 2010). In this study, we successfully established in situ induction of antigen-specific T cell tolerance both in humanized mice and nonhuman primates and examined cellular mechanisms with which DC-based T cell tolerance is achieved.

RESULTS

Development of an immune-modulating anti–human ICAM-1 antibody

To localize the MD-3–binding site in ICAM-1, a series of domain-based fusion constructs with human and mouse ICAM-1 genes were generated and then expressed in HEK293 cells. Individual transfectants were analyzed to identify the MD-3 antibody–binding site in the extracellular domain of the ICAM-1 molecule. The results of flow cytometric analysis showed that MD-3 bound to domain 2 of ICAM-1 (Fig. 1 A).

ICAM-1 mediates leukocyte–leukocyte and leukocyte–endothelial interactions by binding to LFA-1 (lymphocyte function–associated antigen 1) and Mac-1 (Dustin et al., 1986). Thus, some antibodies directed against ICAM-1 or LFA-1 could block leukocyte adhesion to endothelial cells (Smith et al., 1988) and T cell activation (Sanchez-Madrid et al., 1982), resulting in prolongation of allograft survival (Badell et al., 2010). Particularly, some antibodies against domain 2 of ICAM-1 such as R6-5-D6 could inhibit LFA-1 adhesion, although the LFA-1–binding site is located in domain 1 of ICAM-1 (Berendt et al., 1992). Therefore, we investigated whether the adhesion of leukocytes to human umbilical vein endothelial cells (HUVECs) was affected by MD-3

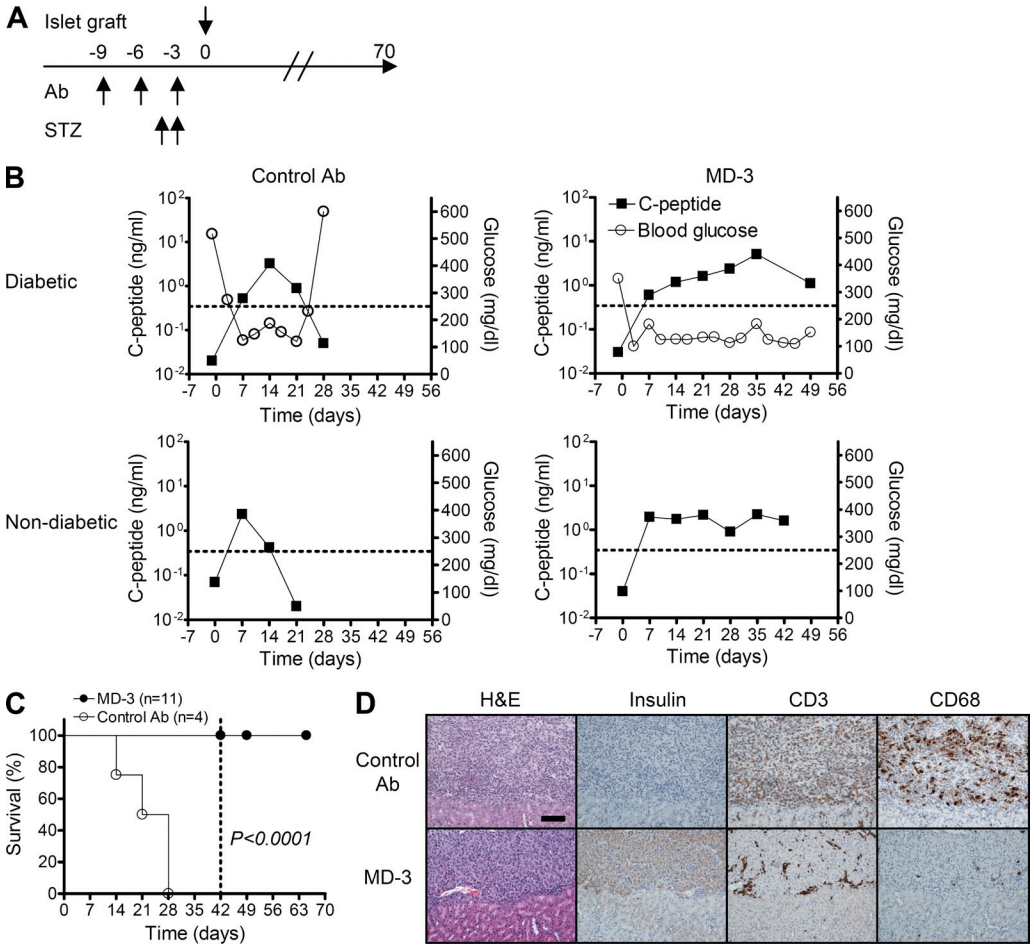

Figure 3. Assessment of graft survival in humanized mice. Porcine islets were transplanted under the renal capsule of humanized mice that had been rendered diabetic by STZ or were nondiabetic and received an injection of isotype-matched irrelevant control or MD-3 antibody (Ab). (A) Experimental protocol. (B) Fasting blood glucose (open circles; right y axis) and porcine C-peptide (closed squares; left y axis) levels were monitored weekly. (C) Based on serum level of porcine C-peptide, functional survival of islet xenografts was plotted over time. The dotted line indicates the day when a portion of the mice were sacrificed for ELISPOT and histopathological analyses. (D) Serial kidney sections of a representative mouse in the control or MD-3–treated groups were stained with H&E or antibodies specific for insulin, human CD3, or human CD68. Bar, 100 µm.

(Fig. 1 B). Unlike anti-CD18 antibody (IB4) and R6-5-D6, which inhibited the adhesion of peripheral blood leukocytes to HUVECs, MD-3 did not affect these adhesions.

In situ induction of antigen-specific T cell tolerance by MD-3 treatment in humanized mice

To investigate the induction of T cell tolerance, we established a porcine islet xenograft model in humanized mice, which were properly repopulated with human immune cells (Fig. 2). In these mice, T and B cells were fully repopulated ~14–16 wk after i.v. injection of human cord blood $CD34^+$ cells (Fig. 2 B). Diabetes was induced through two injections of streptozotocin (STZ; total dose, 200 mg/kg) before transplantation. Control animals received an irrelevant IgG1 monoclonal antibody, and the experimental group received MD-3. These two antibodies were injected into mice three times at 3-d intervals (dose 300 μg per mouse) before islet transplantation (Fig. 3, A and B [top]). Humanized mice that did not receive STZ before porcine islet transplantation were also examined to exclude any possible effect of STZ on MD-3 antibody function and generalized immune response (Fig. 3 B, bottom). Blood glucose and serum porcine C-peptide levels were monitored weekly (Fig. 3 B), and mice were sacrificed 42 d after the initial transplantation (Fig. 3 C).

Median graft survival in the control group was 24.5 d. In contrast, animals treated with MD-3 showed no evidence of graft rejection up to the time of their sacrifice at 42 d (Fig. 3, B and C). In the control group, insulin-positive porcine islet cells were completely destroyed and replaced by inflammatory infiltrates, in which $CD3^+$ T cells and either $CD68^+$ macrophages were the predominant cellular components (Fig. 3 D, top). In contrast, in the MD-3–treated group, large nests of insulin-positive porcine islet cells were clearly seen in the subcapsular area of the kidney with negligible infiltration of mononuclear cells in the peri-islet area (Fig. 3 D, bottom).

Although MD-3 treatment resulted in the prolonged survival of xenografts in humanized mice, it was unclear whether the lack of an immune response was a result of antigen-specific or generalized immunosuppression. To address this, we selected two third-party stimulating antigens: a cellular alloantigen and soluble KLH. When total splenocytes from control mice were stimulated with porcine islets, significant numbers of IL-2– and IFN-γ–secreting T cells were detected (Fig. 4, A and B, left). In contrast, IL-2– and IFN-γ–secreting T cells were almost completely absent from MD-3–treated mice, indicating the complete suppression of T cell responses to xenoantigens. In this system, the activation of T cells in response to human alloantigens, as assessed by mixed lymphocyte reaction (MLR), was comparable with that of controls (Fig. 4, A and B, middle). These data suggest that the unresponsiveness of the T cells does not reflect generalized immunosuppression, but rather the induction of T cell tolerance specific for porcine islet antigens. This induction of antigen-specific T cell tolerance was further indicated by in vivo challenge with an unrelated soluble antigen, KLH. At day 28 after transplantation, at which time MD-3 had been cleared completely, mice were immunized with soluble KLH antigen. 2 wk later, splenocytes were isolated and restimulated with the same antigen in an ex vivo system, and the numbers of KLH-specific T cells were evaluated in an ELISPOT assay. As shown in Fig. 4 (A and B, right), there was a clear anti-KLH response in MD-3–treated mice in terms

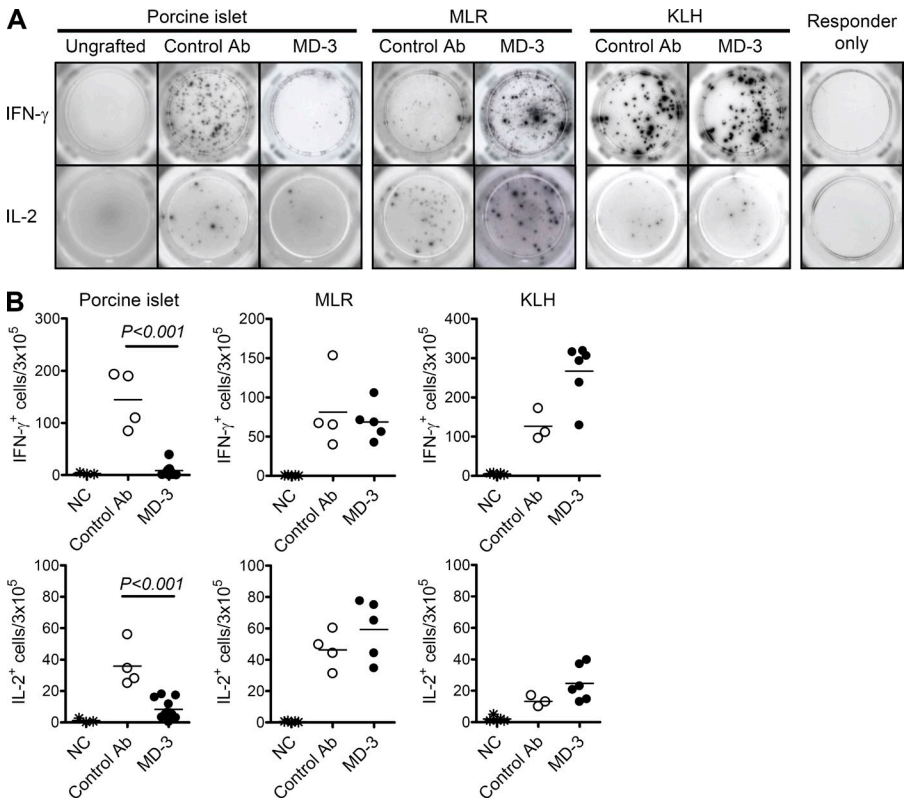

Figure 4. Induction of antigen-specific T cell tolerance in humanized mice. To assess antigen-specific T tolerance in humanized mice that received the islet graft, some recipient mice were challenged with KLH at 4 wk after transplant. Splenocytes were isolated at 6 wk after transplant and tested for recall IL-2 and IFN-γ responses against donor islets, human allogeneic blood mononuclear cells (MLR), and KLH by ELISPOT assay. (A) Representative results. (B) Summarized data from 4–11 mice are presented as total numbers of cytokine-producing cells per 3×10^5 splenocytes. As a negative control (NC) for anti-islet response, splenocytes from humanized mice that did not undergo transplantation (ungrafted) were stimulated with porcine islets. In contrast, splenocytes from engrafted mice cultured in the absence of stimulating antigen (responder only) were used as a negative control for MLR and anti-KLH responses. Horizontal bars represent mean values. Ab, antibody.

of the numbers of cells producing IFN-γ and IL-2. These data again suggest that a normal immune response to KLH occurred in humanized mice that had been tolerized against diverse antigens from grafted porcine islets, indicating that the response was antigen specific.

MD-3 treatment arrests human DCs in a semimature stage in vitro and in vivo

We next investigated whether MD-3 could modulate the maturation status of human monocyte-derived DCs. Human $CD14^+$ monocytes, isolated as precursors of monocyte-derived DCs, were incubated for 6 d with GM-CSF and IL-4, in the presence of MD-3 or a control antibody, to induce their differentiation into immature DCs. Subsequently, immature DCs were treated with the Toll-like receptor agonist, LPS (maturation signal), for 1 d and then analyzed for cytokine production and surface expression of molecules linked to antigen presentation. As shown in Fig. 5 (A and B), treatment of monocytes with MD-3 from the beginning of culture resulted in the arrest of DC maturation in a semimature state. This differentiation state was confirmed by the expression of surface molecules, such as MHC classes I & II, CD80, CD86, and CD40, at levels between those of immature and mature DCs (Fig. 5 A). Furthermore, the production of cytokines, notably IL-12p70, IFN-γ, IL-6, and TNF, was significantly lower in MD-3–treated cells than in those treated with the control antibody (Fig. 5 B). The phenotype and function of DCs treated with MD-3 during their maturation were consistent with the features of semimature or tolerogenic DCs (Morelli and Thomson, 2007). Thus, these in vitro results suggest that MD-3 alone can arrest DC maturation in a semimature state.

Next, to analyze the effect of MD-3 on DC maturation status in vivo, we injected MD-3 and control antibodies into humanized mice three times at 3-d intervals and then treated them with LPS. At 24 h after LPS treatment, DCs in spleens were analyzed for surface expression of CD80 and CD86 (Fig. 5 C, left and middle), and their numbers in control and MD-3–treated groups were compared (Fig. 5 C, right). As anticipated, the expression of both surface molecules was reduced in DCs from MD-3–treated mice versus the control group (Fig. 5 C). These in vivo results, together with the aforementioned in vitro data, suggest that this form of maturation arrest could be achieved through in vivo treatment with MD-3 alone.

Because ICAM-1 is expressed on vascular endothelial cells, as well as activated T and B cells, we next determined (a) whether there are any changes in the surface expression of MHC and co-stimulatory molecules and the production of inflammatory cytokines in HUVECs and activated T cells and (b) antibody production in activated B cells, when treated with MD-3 antibody. In HUVECs, we were not able to see any differences in surface expression and cytokine production of control and

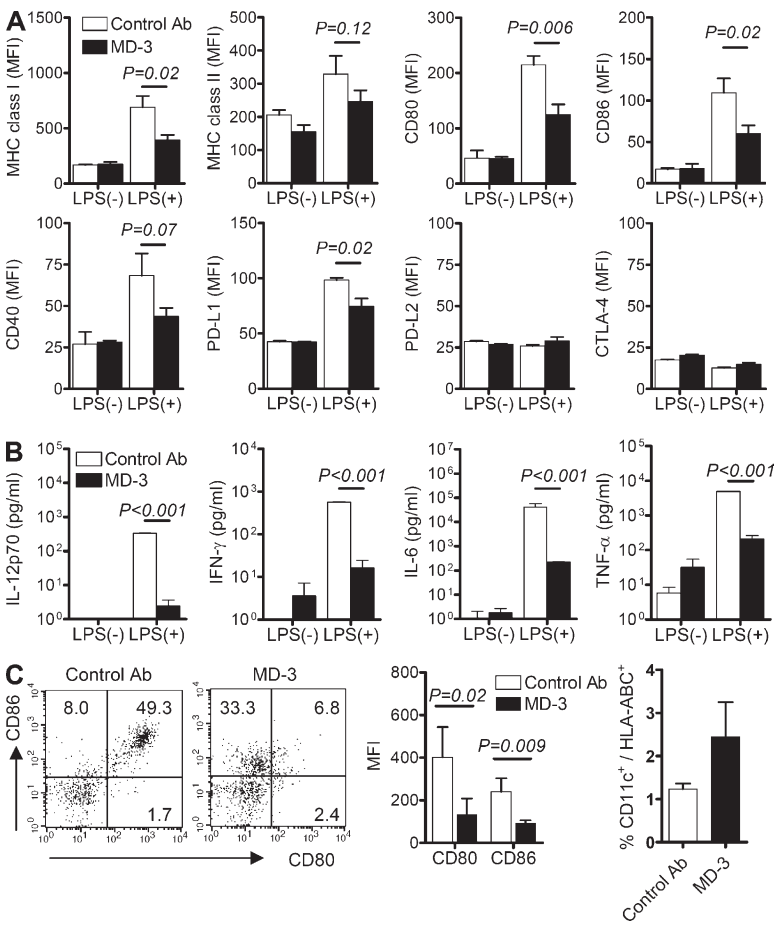

Figure 5. Arrest of DC maturation at the semimature stage. Immature monocyte-derived DCs were generated from human $CD14^+$ monocytes by incubation with GM-CSF and IL-4 in the presence of MD-3 or isotype-matched control antibody (control Ab) from the beginning of culture. After 6 d, DCs were stimulated or not with LPS. (A) Expression levels of MHC class I and II, CD80, CD86, CD40, PD-L1, PD-L2, and CTLA-4 on their surface were compared by flow cytometry. Cumulative data showing mean fluorescent intensity (MFI) ± SE of MHC class I and II, CD80, CD86, and CD40 were obtained from four independent experiments. Data showing mean fluorescent intensity ± SE of PD-L1, PD-L2, and CTLA-4 are representative of two independent experiments in triplicate. (B) Representative cytokine levels in the culture supernatants of immature and LPS-treated monocyte-derived DCs in the presence of MD-3 or control antibody. Results are the mean ± SE of triplicate cultures, and data are representative of three independent experiments. (C) Humanized mice received MD-3 or control antibody three times before LPS (100 µg/mouse) administration. Splenocytes were isolated 1 d after LPS injection and stained with HLA-ABC, CD11c, CD80, and CD86 antibodies. Representative dot plots of CD80 and CD86 expression on gated $CD11c^+$ DCs are shown at the left. Numbers indicate the percentage of cells in each quadrant. Cumulative data ($n = 3$) showing mean fluorescent intensity were obtained from three independent experiments (middle). The percentages of $CD11c^+$ cells among $HLA\text{-}ABC^+$ cells in spleens were also calculated (right). Error bars indicate SE.

MD-3–treated groups (not depicted). This was also the case in activated T cells in terms of T cell proliferation and cytokine production (not depicted). Finally, LPS-treated B cells did not show any differences in total Ig secretion (not depicted).

DCs play a major role in MD-3–induced antigen-specific T cell tolerance

To confirm that DCs play a key role in the induction of antigen-specific tolerance in vivo, we established a modified mouse model system in which DCs were almost completely depleted by the systemic administration of saporin-conjugated anti-CD11c immunotoxin (IT; Fig. 6 A). Before porcine islet transplantation, MD-3 was administered three times to humanized mice in two different groups, one of which received anti-CD11c IT at 2-d intervals (Fig. 6 A). As shown in Fig. 6 B, intraperitoneal injection of anti-CD11c IT nearly completely ablated DCs in humanized mice up to 10 d after islet graft. Serum MD-3 levels were measured two times per week, and MD-3 was not detected at 7 d after transplantation. At 12 d after transplantation, both groups of humanized mice were immunized with a mixture of alum and KLH. Importantly, 26 d after transplantation, numbers of IL-2– and IFN-γ–secreting T cells after rechallenge of porcine islet cells ex vivo differed significantly between control and DC-ablated mice. Ablation of $CD11c^+$ DCs at the time of xenoantigen challenge resulted in severe impairment of T cell tolerance, whereas mice treated with MD-3 alone mounted a T cell tolerance to xenoantigen challenge (Fig. 6 C, left).

Next, we examined whether the T cell response that had returned against islet antigens was caused by the recovery of a normal immune response, which had been lost via the ablation of DCs. To that end, we assessed T cell responses to KLH in both mouse groups. Both groups exhibited clear T cell responses to KLH (Fig. 6 C, middle). However, in these experiments, numbers of KLH-responding T cells were reduced in anti-CD11c IT–treated mice, probably because of actual decreases in the numbers of DCs present in their spleens (Fig. 6 D), suggesting that there may still have been a low level of toxicity. To normalize the anti-islet immune response based on the individual immune status of the mouse, we divided the number of islet-responding T cells by the number of spots responding to KLH stimuli in each mouse and expressed the relative value as a percentage. The data obtained demonstrated a clear difference in the T cell response to islet antigens between the two groups (Fig. 6 C, right). These results indicate that the induction of antigen-specific T cell tolerance depends primarily on DCs.

MD-3 efficiently induces antigen-specific T cell tolerance in nonhuman primates

Although humanized mice are powerful tools for exploring the functions of T and B cells and DCs, there are certain limitations when extrapolating humanized mouse data to humans. This includes the lack of granulocytic series, NK cells, and other as of yet unidentified factors (Shultz et al., 2007). Fortunately, similar to the human system, MD-3 antibody binds to domain 2 of Rhesus ICAM-1 (Fig. 7 A). Therefore, to test whether data from the humanized mouse system could be reproduced in a nonhuman primate model, we conducted the same analyses in Rhesus macaques.

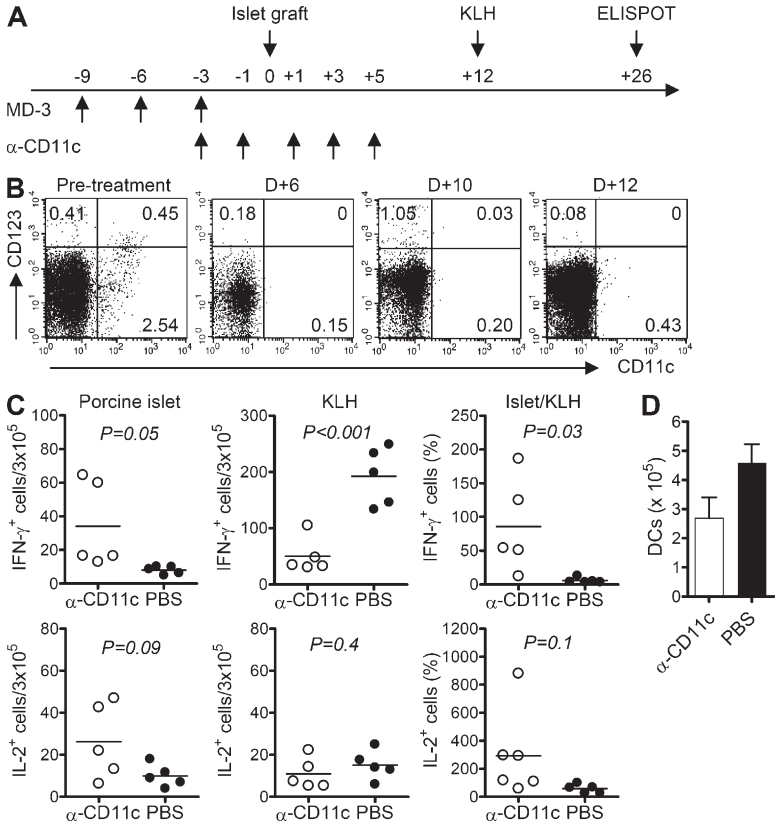

Figure 6. Abrogation of T cell tolerance induction after DC ablation. Humanized mice received anti-CD11c IT (α-CD11c; 5 µg/mouse) or PBS every other day from 3 d before porcine islet transplantation up to the fifth day after transplant (D+5). These mice were then immunized with KLH on the 12th day after transplant (D+12). (A) Experimental scheme. (B) Flow cytometric analysis on the indicated days after islet transplantation to assess depletion of $CD11c^+$ DCs in the spleen of humanized mice. (C) Splenocytes were isolated 14 d after KLH immunization and tested for recall IL-2 and IFN-γ responses via ELISPOT assay against donor islets and KLH. The data from individual mice are presented as total numbers of cytokine producing cells per 3×10^5 splenocytes or normalized anti-islet response (Islet/KLH) by dividing the anti-islet spot number by the anti-KLH spot number in each mouse. Horizontal bars represent mean values. (D) Splenocytes from each mouse were stained with anti–human CD11c and anti–HLA-ABC antibodies, and the total number of $CD11c^+$ DCs was calculated after flow cytometric analysis. Error bars indicate SE.

Rhesus macaques, in which diabetes had been induced through the injection of STZ, underwent i.v. glucose tolerance testing to confirm the absence of insulin and C-peptide production before porcine islet cell transplantation. Recipient monkeys (R043, R042, and R038) were treated with MD-3 alone before intraportal injection of porcine islets (50,000 islet equivalents [IEQs]/kg). MD-3 monotherapy failed to achieve graft survival for >8 d, whereas ELISPOT analysis of PBMCs isolated from three recipient monkeys revealed near-complete suppression of IFN-γ and IL-2 responses to donor pig islet antigen from day 7–47 (Fig. 7 B), clearly indicating the induction of T cell tolerance to porcine islets. However, long-term graft survival was finally achieved with a combination treatment of low-dose rapamycin (trough level 6–12 μg/ml) and mouse–human IgG1 chimeric anti–human CD154 blocking antibody (5C8 clone derivative; National Institutes of Health Nonhuman Primate Reagent Resource), as well as MD-3. This combined therapy of rapamycin and chimeric ant-CD154 antibody were known to regulate NK and NK-mediated innate B cell activation, which has been reported to be related to T-independent antigens, such as galactose-α-1,3-galactose (Gal) and non-Gal sugar antigens (Li et al., 2007; Eissens et al., 2010). This protocol prolonged the graft survival to >140 d as indicated by a normal blood glucose level and sustained high level of porcine C-peptide (Fig. 8 A). Importantly, these two monkeys (R052 and R049) again maintained xenoantigen-specific T cell tolerance as shown by suppression of IFN-γ and IL-2 responses to donor pig islet antigens, whereas an intact immune response to a third party of alloantigen was maintained (Fig. 8 B).

DISCUSSION

For more than the past two decades, various monoclonal antibodies that block interactions between co-stimulatory molecules and their ligands on T cells have been developed to control unwanted immunological reactions (Ford and Larsen, 2009). However, a major problem of using these tools is that they cause generalized immunosuppression rather than antigen-specific T cell tolerance. In this study, we successfully established in situ induction of antigen-specific T cell tolerance and dissected the cellular mechanisms underlying these findings.

MD-3 binds to the second domain of human ICAM-1. When Toll-like receptors on DCs bind LPS in the presence of MD-3, the DCs are not fully mature and express cell surface molecules linked to antigen presentation at levels intermediate between those in immature and fully mature DCs. Importantly, the cytokine profiles of control and MD-3–treated groups showed even greater differences (>100-fold). A few previous studies have shown that stable T cell contacts are required for full activation, whereas repeated brief DC–T cell interactions are characteristic of induction of T cell tolerance (Hugues et al., 2004; Shakhar et al., 2005). Based on these findings, MD-3–mediated induction of semimature DCs seems to result in both a short duration of DC–T cell interaction and a shortage of cytokines, and thereby induction of T cell tolerance. The possibility that tolerance induction was caused by a defect in transendothelial migration can be ruled out by the findings of a cell adhesion assay, which revealed no difference in adhesion activity between

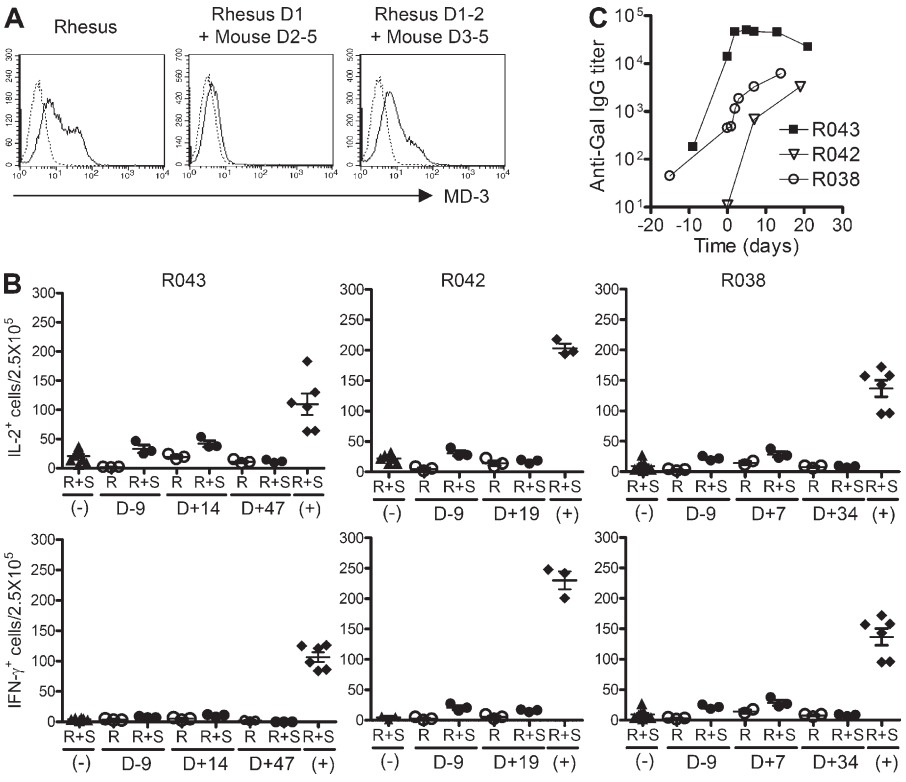

Figure 7. Induction of T cell tolerance in a nonhuman primate. (A) HEK293 cells were transfected with Rhesus *ICAM1* gene or chimeric genes of Rhesus and mouse ICAM-1, and MD-3 binding was assessed by flow cytometry (solid line). As the negative control (dotted line), the cells were stained with only FITC-conjugated secondary antibody. (B) Adult porcine islets (50,000 IEQs/kg) were intraportally transplanted into three Rhesus monkeys (R043, R042, and R038) that received MD-3 antibody alone. PBMCs were isolated on the indicated days after transplantation, and the frequency of T cells secreting IL-2 or IFN-γ in response to donor islets was determined by ELISPOT assay. Results are presented as numbers of cytokine-producing cells per 2.5 × 10^5 PBMCs in each triplicate culture. R, responder cells only; R+S, responder cells stimulated with porcine islet cells; (−), negative control responder cells from unsensitized monkeys stimulated with porcine islet cells; (+), positive control responder cells from sensitized monkeys stimulated with porcine islet cells. Error bars indicate SE. (C) Anti-Gal IgG levels were measured at the indicated time before and after porcine islet transplantation via ELISA.

control and MD-3–treated cells. In addition, inhibitory signaling through the interaction of PD1 and PD-L1/L2 and CTLA-4 and B6 appears not to play a major role in our system, as the expression levels of PD-L1, PD-L2, and CTLA-4 were not higher in MD-3–treated DCs, as compared with control (Fig. 5 A).

In in vitro experiments, MD-3 treatment resulted in the generation of semimature DCs. A similar response was observed in vivo after the sequential injection of MD-3 and LPS. To determine whether the in vivo induction of T cell tolerance was mediated primarily by DCs, we developed a mouse model system in which DCs were almost completely ablated by i.v. injection of saporin-conjugated anti-CD11c IT. Tolerance induction did not occur in this system. These data clearly indicate that MD-3–induced tolerance was mediated by DCs.

There is increasing evidence that DCs are charged with maintaining tolerance to self or innocuous antigens, the failure of which can lead to autoimmune and/or inflammatory diseases (Aichele et al., 1994; Hawiger et al., 2001; Fu and Jiang, 2010). Because of their pivotal role in controlling tolerance responses, DCs have emerged as strong candidates for modulating the immune system in an antigen-specific manner and as targets for immunotherapy for diverse conditions (Tarner et al., 2003; van Duivenvoorde et al., 2006; Steinman and Banchereau, 2007; Tarbell et al., 2007; Zahorchak et al., 2007). Numerous strategies have been devised to generate stable tolerogenic DCs, including their modification with chemicals (Buckland and Lombardi, 2009), cytokines (Torres-Aguilar et al., 2010), peptides (Delgado, 2009), and immunosuppressive drugs (Turnquist et al., 2007), as well as gene modification (Tan et al., 2005). Most of these strategies have focused on the maturation of DCs in vitro under specific culture conditions and the subsequent i.v. injection of tolerogenic DCs to induce T cell tolerance. This method for inducing tolerogenic DCs in vitro shows fairly good effects in some cases (Tarbell et al., 2007; Zahorchak et al., 2007). However, it would be preferable if we could induce tolerance

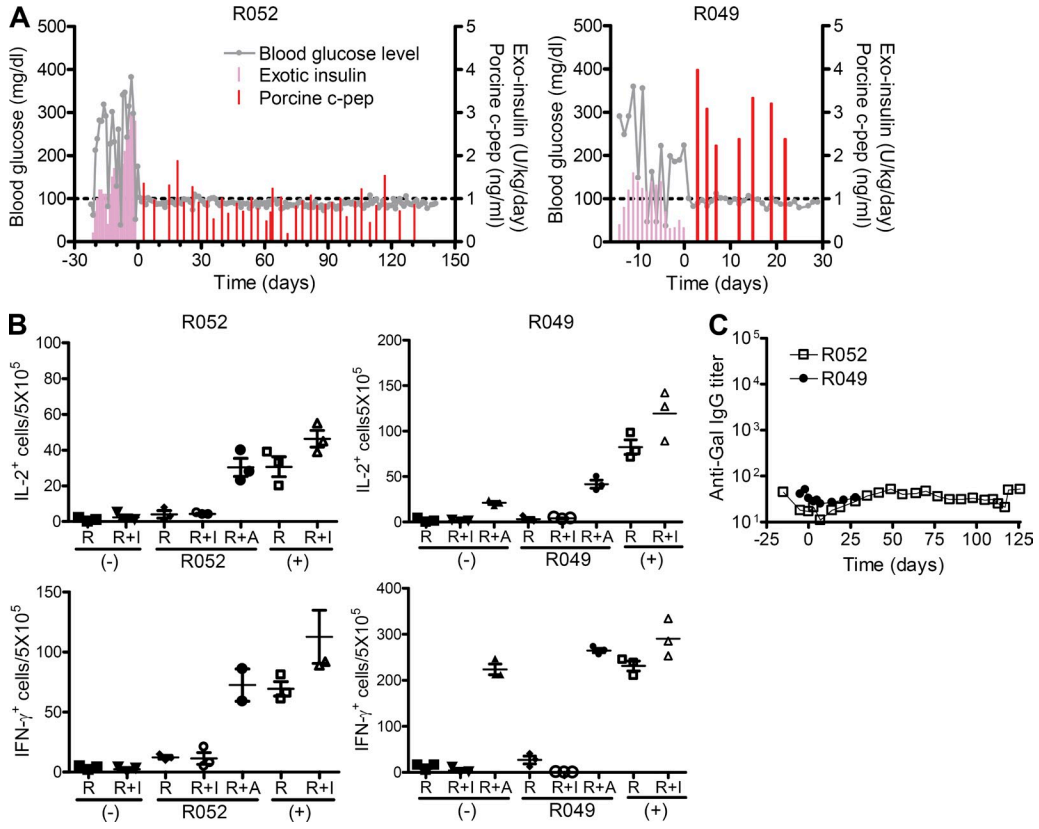

Figure 8. Achievement of long-term survival of a porcine islet xenograft in a nonhuman primate via combination therapy including MD-3. (A) After successfully inducing type 1 diabetes in Rhesus monkey via STZ administration, hyperglycemia was controlled by s.c. injecting human recombinant insulin (Exotic insulin). Adult porcine islets (100,000 IEQs/kg) were intraportally transplanted into Rhesus monkeys (R052 and R049) that received MD-3 combined with rapamycin and anti-CD154 antibody. Blood glucose level and serum porcine C-peptide concentration were measured at the indicated time after porcine islet transplantation. (B) PBMCs were isolated at 127 and 7 d after transplantation from R052 and R049, respectively, and the frequency of T cells secreting IL-2 or IFN-γ in response to donor islets (I) or allogeneic PBMCs (A) was determined by ELISPOT assay. Results are presented as numbers of cytokine-producing cells per 5×10^5 PBMCs in each triplicate culture. R, responder cells only; R+I, responder cells stimulated with porcine islet cells; R+A, responder cells stimulated with allogeneic PBMCs; (−), unsensitized monkeys as a negative control; (+), sensitized monkeys as a positive control. Error bars indicate SE. (C) Anti-Gal IgG levels were measured at the indicated time before and after porcine islet transplantation via ELISA.

status in an in vivo system without the need for in vitro manipulation of DCs (Morelli and Thomson, 2007). In this respect, a major advantage of using MD-3 is that, as we have shown, in vivo challenge with this antibody resulted in the in situ generation of semimature DCs and subsequent induction of antigen-specific T cell tolerance.

Because it is important to evaluate the effects of MD-3 under conditions that more closely mimic human physiology, we tested whether MD-3 was also able to induce T cell tolerance in Rhesus macaques. Porcine pancreatic islets were transplanted intraportally into monkeys that had been administered MD-3 three times before transplantation. Although MD-3 alone cannot achieve long-term graft survival, it efficiently induced T cell tolerance against porcine islet antigens as shown by ELISPOT analysis. We speculated that the rejection would be mediated by antibodies against thymus-independent carbohydrate antigen as the monkeys exhibited early rapid rising of anti-Gal IgG levels (Fig. 7 C). A previous study reported that rapidly induced T cell–independent xenoantibody production is mediated by marginal zone B cells and requires help from NK cells via the CD40–CD40L interaction (Li et al., 2007). By using MD-3 with a combination of anti-CD154 antibody and rapamycin, which is known to inhibit NK-mediated cytotoxicity, we were able to achieve porcine islet graft survival for >140 d by now. In addition, in these recipients, we observed no increases in Gal-specific IgG antibody levels after transplant (Fig. 8 C).

In this study, we demonstrated that MD-3 treatment induced antigen-specific T cell tolerance against grafted antigens rather than generalized immunosuppression. The present data raise the possibility that the administration of MD-3 may also be able to induce T cell tolerance to all types of antigens within the recipients, including latent viruses such as Epstein-Barr virus. This possibility should be considered in a clinical trial. However, during latency, viral genes are incorporated into the host chromosome, and viral antigens are not able to be efficiently presented to T cells. Therefore, host T cells appear not to be tolerized to these viral antigens during this latent stage, during the time recipients are treated with MD-3.

The mechanism of how ICAM-1 signaling can handle DCs for their maturation has never been shown before. This work is now under way in this laboratory.

In summary, we were able to induce in situ antigen-specific T cell tolerance in an in vivo system. MD-3, a unique monoclonal antibody that recognizes domain 2 of human ICAM-1, efficiently induced the differentiation of immature DCs into semimature DCs both in vitro and in vivo. This induction of T cell tolerance is particularly meaningful because it was highly specific for target antigens. Therefore, MD-3–induced tolerance is a highly promising strategy for the prevention of transplant rejection.

MATERIALS AND METHODS

Animals. NOG mice were obtained from the Central Institute for Experimental Animals (Kawasaki, Japan). The donor pigs, Seoul National University (SNU) miniature pigs (Kim et al., 2009), were bred in a barrier-sustained specific pathogen-free facility. Mice and pigs were maintained under specific pathogen-free conditions at the animal facility of the Center for Animal Resource Development, SNU College of Medicine. Experiments were performed after receiving approval from the Institutional Review Board of SNU College of Medicine and the Institutional Animal Care and Use Committee of the Institute of Laboratory Animal Resources, SNU. Islet recipients were Rhesus macaques (*Macaca mulatta*) maintained at the SNU Hospital Non-human Primate Center. The age of the recipients ranged from 48 to 60 mo, and their weight ranged from 4.5 to 5.5 kg. This study was conducted as approved by the SNU Hospital Animal Care and Use Committee and according to the National Institutes of Health guidelines.

Development of anti–human ICAM-1 monoclonal antibody and mapping of its binding domain. A hybridoma cell line producing the MD-3 monoclonal antibody was generated by fusing splenocytes from BALB/c mice immunized with human ICAM-1/Fc fusion proteins and SP2/0-Ag14 myeloma cells. To identify the *ICAM1* domain for MD-3 antibody binding, human and mouse *ICAM1* genes were obtained from N. Hogg (Cancer Research UK, London, England, UK). The monkey ICAM-1 gene was cloned based on the published sequence (available from GenBank/EMBL/DDBJ under accession no. NM_001047135.1). The chimeric constructs were cloned according to a previously described protocol (Berendt et al., 1992). HEK293 cells transfected with plasmid DNA were stained with primary antibody at 4°C for 30 min. After washing in PBS with 0.05% Tween 20 and staining with FITC-conjugated anti–mouse Ig antibody at 4°C for 30 min, the live cells, gated as the propidium iodide (Sigma-Aldrich)–negative population, were analyzed using FACSCalibur (BD) equipped with CellQuest Pro software (BD).

Generation of monocyte-derived DCs. Human $CD14^+$ monocytes were isolated from healthy volunteers using magnetic sorting, and immature DCs were derived from purified monocytes by culture with 1,000 U/ml GM-CSF (PeproTech) and 1,000 U/ml IL-4 (PeproTech) in the absence or presence of 10 μg/ml of antibodies, as described previously (Subklewe et al., 1999), and were matured on day 6 by adding 5 μg/ml LPS (Sigma-Aldrich) after washing. The next day, the cells were harvested for flow cytometry, and the cytokine concentration in the culture supernatant was measured by Cytometric Bead Array (BD). The following fluorochrome-labeled monoclonal antibodies were purchased from BD or Dinona: anti–human MHC class I (YG13), MHC class II (L243), CD11c (B-ly6), CD80 (L307.4), C86 (FUN-1), CD40 (5C3), PD-L1 (MIH1), PD-L2 (MIH18), and CTLA-4 (BNI3).

Generation of humanized mice. Humanized mice were generated according to a previously described protocol (Ito et al., 2002). NOG mice were exposed to 200 rad of total body irradiation from a ^{137}Cs source. The next day, each recipient mouse received 1–2 × 10^5 $CD34^+$ cells that were purified from human cord blood cells using magnetic sorting (Miltenyi Biotec). Repopulation of total human hematopoietic cells and T cells in peripheral blood was monitored weekly by flow cytometry after staining with anti–human MHC class I and CD3 antibodies. At the time of sacrifice, spleens were collected, and single cells were resuspended in flow cytometry buffer (PBS with 0.1% bovine serum albumin and 0.1% Na azide). After staining with fluorochrome-conjugated antibodies for 30 min at 4°C, the live cells were analyzed using a flow cytometer. The following fluorochrome-labeled monoclonal antibodies were purchased from BD or Dinona: anti–human MHC class I (YG13), CD3 (UCHT1), CD4 (RPA-T4), CD8 (DN17), CD11c (B-ly6), CD14 (MEM-18), CD15 (HI98), CD19 (HIB19), CD80 (L307.4), C86 (FUN-1), and CD123 (9F5).

Porcine pancreas procurement and islet isolation. A total pancreatectomy was performed without warm ischemia time, and islet isolation was performed using the modified Ricordi method, as previously described (Jin et al., 2010). In brief, Liberase MTF C/T (Roche) or CIzyme collagenase MA and CIzyme BP protease (VitaCyte) were dissolved in endotoxin-free

water and diluted to a total volume of 1 ml/g of pancreas weight with a preservation solution at 4°C and intraductally administered. The preservation solution was composed of Na hydroxide, potassium hydroxide, calcium chloride, magnesium sulfate, Na phosphate, D-mannitol, and NaCl. During digestion, the pancreas, which was inflated with collagenase, was incubated without shaking for 12–15 min at 35–37°C until the pancreas tissue was loosened. This was followed by manual shaking with serial sampling. After free islets were observed in the serial sample, digestion was stopped by cooling to 4°C and exposing the islets to 10% porcine serum. Islets were purified with a continuous OptiPrep density gradient (Axis-Shield) and a Cobe 2991 cell separator (Gambro BCT Inc.). Purified islets were cultured overnight in Medium 199 (Invitrogen) supplemented with 10% porcine serum, 10 mM nicotinamide (Sigma-Aldrich), and 1% penicillin-streptomycin at 37°C.

Porcine islet grafts in humanized mice. Diabetes was induced by high-dose i.v. STZ (total of 200 mg/kg, split into two doses separated by 24 h), and mice with fasting glucose levels >250 mg/dl were considered diabetic. 7 d later, isolated porcine islets (5,000 IEQs/mouse) were transplanted under the kidney capsule. Peripheral blood was sampled weekly from the retroorbital sinus to monitor blood glucose levels using a portable glucometer (Accu-Chek; Roche), and porcine C-peptide levels in serum were determined by radioimmunoassay (Linco) according to the manufacturer's protocol. A successful engraft was defined as porcine C-peptide >0.5 ng/ml, and graft rejection was defined as the day of C-peptide <0.1 ng/ml. Rejection was confirmed by histological analysis of the grafts.

Induction of type 1 diabetes in nonhuman primates. A central venous catheter (5Fr. Dual-Lumen PICC; Bard Access System) was inserted into the right internal jugular vein in monkeys under general anesthesia. Monkeys were fasted overnight and were prehydrated with normal saline (0.9% NaCl, 40–60 ml/kg/day i.v.) via a tether system for 12 h before STZ (USB Co.) administration to reduce adverse nephrotoxic effects. Butorphanol or metoclopramide was also administered to prevent chemically induced vomiting caused by the STZ. A high dose of STZ (110–120 mg/kg) was diluted with 10 ml normal saline and given i.v. within 5 min. Additional hydration with normal saline was given for 2–4 h. Blood glucose levels were measured using a portable glucometer (Accu-Chek) or a continuous glucose monitoring system (Guardian RT; Medtronic Inc.). STZ was administered in the morning, and a light meal was given to the monkeys in the afternoon. If there was a loss of appetite, dextrose was infused via a tether system to prevent hypoglycemia. Liver and kidney function tests were performed before and after STZ administration, and C-peptide levels were assessed by radioimmunoassay (Linco) according to the manufacturer's protocol. After successfully inducing type 1 diabetes, blood glucose levels were checked at least two or three times per day, and hyperglycemia was controlled by s.c. injecting human recombinant insulin such as Humalog (Eli Lilly), Novolin N (Green cross), or Lantus (Sanofi-Aventis). Fasting and nonfasting blood glucose levels were maintained in the diabetic monkeys at approximately <150 mg/dl (>8.3 mmol/l) and <200 mg/dl (11.1 mmol/l), respectively. Complete type 1 diabetes was confirmed by persistent hyperglycemia and <0.2 ng/ml of C-peptide levels based on the i.v. glucose tolerance test. In brief, after an overnight fast and no insulin, 0.5 g/kg of 50% dextrose solution added to same volume of normal saline was infused i.v. for 1 min. Blood glucose levels were measured in monkeys before and 2, 5, 15, 30, 60, 90, and 120 min after infusion. Insulin and C-peptide levels were measured at the same time intervals.

Islet transplantation into nonhuman primates. All monkeys were fasted for 12 h before surgery. After premedicating the monkeys with atropine sulfate (0.04 mg/kg s.c.; Huons), general anesthesia was induced with thiopental Na (25 mg/kg i.v.; JWP) and maintained with 1% isoflurane, N_2O, and O_2. Lactated Ringer's solution or 5% dextrose saline was administered i.v. during the operation. Cefazolin Na (25 mg/kg i.v.; Chong Kun Dang) was given prophylactically, and meloxicam (0.2 mg/kg i.v.; Boehringer Ingelheim) was administered for antiinflammatory and analgesic effects before surgery. A laparotomy was performed, and the jejunal arch was exposed to infuse the islets. A 24- or 22-gauge catheter was inserted through the jejunal vein and approached near the portal vein. The porcine islets were infused with gravity pressure for 8–12 min. After infusion, the vessel was ligated with a 5-0 Prolene suture. Finally, the abdominal cavity was closed using a common method. After surgery, the tether system was applied for continuous fluid therapy and infusion of low dose sugar, if necessary.

ELISPOT assay. The frequencies of IL-2– or IFN-γ–secreting antigen-specific T cells in spleens of humanized mice and peripheral blood of nonhuman primates were measured using an ELISPOT kit (Mabtech). Anti–IL-2 or IFN-γ capture antibody-coated plates were washed four times with sterile PBS (200 µl/well) and blocked for 30 min with 10% human serum–supplemented RPMI 1640 media at room temperature. After removing the media, 3×10^5 splenocytes from the humanized mice or 2.5×10^5 of PBMCs from nonhuman primates were cultured with 5×10^4 porcine islet cells in RPMI 1640 media supplemented with 10% human serum for 40 h at 37°C in a 5% CO_2 incubator. For humanized mice, 0.1 mg/ml KLH or T cell–depleted γ-irradiated 7×10^5 human PBMCs pooled from three volunteers were also used as stimulators. After the 40-h culture, cells were removed, and the plates were washed five times with PBS (200 µl/well). Alkaline phosphatase–conjugated detecting antibody diluted at 1:200 or 1:1,000 for IL-2 or IFN-γ, respectively, in 100 µl PBS containing 0.5% fetal bovine serum was then added and incubated for 2 h at room temperature. The plates were washed five times with PBS, and 100 µl BCIP/NBP substrate was added. Color development was stopped by washing with tap water. The resulting spots were counted on a computer-assisted ELISPOT Reader System (AID).

Generation of anti-CD11c IT. To produce the anti–human CD11c antibody–saporin IT, saporin was purchased from Sigma-Aldrich, and saporin conjugation of antibody was performed as described previously with some modifications (McGraw et al., 1994). In brief, anti–human CD11c antibody was activated with *N*-succinimidyl-3-(2-pyridyldithio)-propionate, conjugated with thiolated saporin, and added to *N*-ethylmaleimide to block unreacted sulfhydryl groups. After removing the unconjugated saporin by protein G affinity chromatography, the anti-CD11c–saporin complexes were eluted with ImmunoPure elution buffer (Thermo Fisher Scientific) and dialyzed against PBS. The possibility of contamination by free saporin was ruled out by SDS-PAGE.

Cell adhesion assay. The IB4 monoclonal antibody (anti-CD18) has been previously described (Wright et al., 1983), as has the monoclonal antibody R6-5-D6 against ICAM-1 (Smith et al., 1988; Berendt et al., 1992). HUVECs were prepared and cultured on hydrated collagen gels (for monocyte adhesion) or directly on fibronectin-coated 96-well plates (for neutrophil adhesion), as described previously (Muller et al., 1989). For neutrophil adhesion, HUVEC monolayers were activated by culturing them in 10 ng/ml TNF overnight. HUVECs were not activated for monocyte adhesion assays. Under these conditions, when freshly isolated PBMCs are added, lymphocytes do not stick to the endothelial cells, but monocytes do (Muller and Weigl, 1992). Neutrophils (Lou et al., 2007) and PBMCs (Muller and Weigl, 1992) were isolated as described previously and subjected to adhesion assays using the standard approaches (Muller and Weigl, 1992; Lou et al., 2007; Muller and Luscinskas, 2008). In brief, freshly isolated polymorphonuclear neutrophils or PBMCs were resuspended to 1×10^6 cells/ml or 2×10^6 cells/ml, respectively, mixed gently with monoclonal antibodies at a final concentration of 20 µg/ml, and added to the endothelial monolayers for 25 min at 37°C. Monolayers were washed free of nonadherent cells, fixed, and stained with Wright-Giemsa stain for microscopic evaluation. Six replicates of each variable were performed for each experiment.

Histopathological examination and immunohistochemical staining of tissue sections. Formalin-fixed, paraffin-embedded tissues were sectioned to a thickness of 4 µm and stained with hematoxylin and eosin (H&E). For immunohistochemistry, formalin-fixed, paraffin-embedded tissue sections were dewaxed in xylene, rehydrated using a graded alcohol series, and

incubated in an endogenous peroxide-blocking solution for 5 min. Antigen retrieval was performed by incubating the sections in 6 mM of citrate buffer at 99°C for 20 min using the Bond Max system (Leica), and nonspecific staining was prevented by treating the tissue sections with rabbit serum (1% in PBS) for 30 min. Anti–human insulin (Dako), CD3 (F7.2.38; Dako), and CD68 (PG-M1; Dako) antibodies were applied for 30 min, and antibody binding was detected using a VECTASTAIN Elite ABC kit (PK6101; Vector Laboratories). Microscopic observations were performed with an ECLIPSE 80i Bright-Field Microscope Set (Nikon) equipped with CFI 10×/22 eyepiece, Plan Fluor objectives (with 4×, 10×, 20×, and 100× objectives) and DS-Fi1 camera. We used NIS-Elements BR 3.1 software (Nikon) for image acquisition.

Statistical analysis. All data were analyzed using Prism software (GraphPad Software). Data are presented as mean ± SE. Comparison between groups was performed by either Student's *t* test (two groups) or one-way analysis of variance (multiple groups). Survival data were analyzed by log-rank test. P-values <0.05 were considered significant.

We thank Sang-Man Jin, Kang Seok Kim, and Clifford Carpenter for expert technical assistance, and Dr. Nancy Hogg for the kind gift of ICAM1 gene constructs.

This study was supported by a grant from the Korea Biotech R&D Group of Next-Generation Growth Engine Project of the Ministry of Education, Science and Technology, Republic of Korea (Project no. 2010K001294; to K.C. Jung), a grant from Korea Healthcare Technology R&D Project, Ministry of Health and Welfare, Republic of Korea (Project No.A040004; to C.-G. Park), and grants from the United States National Institutes of Health (R01 HL046849 and R37 HL06774; to W.A. Muller). The anti-CD154 antibody used in these experiments was provided by the National Institutes of Health Nonhuman Primate Reagent Resource (National Institute of Allergy and Infectious Diseases contract HHSN 2722001300031C).

K.C. Jung and S.H. Park are named as co-inventors on a PCT application pertaining to therapeutic effects of MD-3 antibody. The authors have no additional conflicting financial interests.

Submitted: 17 June 2011
Accepted: 29 September 2011

REFERENCES

Aichele, P., D. Kyburz, P.S. Ohashi, B. Odermatt, R.M. Zinkernagel, H. Hengartner, and H. Pircher. 1994. Peptide-induced T-cell tolerance to prevent autoimmune diabetes in a transgenic mouse model. *Proc. Natl. Acad. Sci. USA*. 91:444–448. http://dx.doi.org/10.1073/pnas.91.2.444

Badell, I.R., M.C. Russell, P.W. Thompson, A.P. Turner, T.A. Weaver, J.M. Robertson, J.G. Avila, J.A. Cano, B.E. Johnson, M. Song, et al. 2010. LFA-1-specific therapy prolongs allograft survival in rhesus macaques. *J. Clin. Invest.* 120:4520–4531. http://dx.doi.org/10.1172/JCI43895

Berendt, A.R., A. McDowall, A.G. Craig, P.A. Bates, M.J. Sternberg, K. Marsh, C.I. Newbold, and N. Hogg. 1992. The binding site on ICAM-1 for Plasmodium falciparum-infected erythrocytes overlaps, but is distinct from, the LFA-1-binding site. *Cell*. 68:71–81. http://dx.doi.org/10.1016/0092-8674(92)90207-S

Brehm, M.A., A. Cuthbert, C. Yang, D.M. Miller, P. DiIorio, J. Laning, L. Burzenski, B. Gott, O. Foreman, A. Kavirayani, et al. 2010. Parameters for establishing humanized mouse models to study human immunity: Analysis of human hematopoietic stem cell engraftment in three immunodeficient strains of mice bearing the IL2rgamma(null) mutation. *Clin. Immunol.* 135:84–98. http://dx.doi.org/10.1016/j.clim.2009.12.008

Buckland, M., and G. Lombardi. 2009. Aspirin and the induction of tolerance by dendritic cells. *Handb. Exp. Pharmacol.* 188:197–213. http://dx.doi.org/10.1007/978-3-540-71029-5_9

Chen, Q., M. Khoury, and J. Chen. 2009. Expression of human cytokines dramatically improves reconstitution of specific human-blood lineage cells in humanized mice. *Proc. Natl. Acad. Sci. USA*. 106:21783–21788. http://dx.doi.org/10.1073/pnas.0912274106

Choi, E.Y., W.S. Park, K.C. Jung, D.H. Chung, Y.M. Bae, T.J. Kim, H.G. Song, S.H. Kim, D.I. Ham, J.H. Hahn, et al. 1997. Thymocytes positively select thymocytes in human system. *Hum. Immunol.* 54:15–20. http://dx.doi.org/10.1016/S0198-8859(97)00012-8

Choi, E.Y., K.C. Jung, H.J. Park, D.H. Chung, J.S. Song, S.D. Yang, E. Simpson, and S.H. Park. 2005. Thymocyte-thymocyte interaction for efficient positive selection and maturation of CD4 T cells. *Immunity*. 23:387–396. http://dx.doi.org/10.1016/j.immuni.2005.09.005

Delgado, M. 2009. Generating tolerogenic dendritic cells with neuropeptides. *Hum. Immunol.* 70:300–307. http://dx.doi.org/10.1016/j.humimm.2009.01.020

Dustin, M.L., R. Rothlein, A.K. Bhan, C.A. Dinarello, and T.A. Springer. 1986. Induction by IL 1 and interferon-gamma: tissue distribution, biochemistry, and function of a natural adherence molecule (ICAM-1). *J. Immunol.* 137:245–254.

Eissens, D.N., A. Van Der Meer, B. Van Cranenbroek, F.W. Preijers, and I. Joosten. 2010. Rapamycin and MPA, but not CsA, impair human NK cell cytotoxicity due to differential effects on NK cell phenotype. *Am. J. Transplant.* 10:1981–1990. http://dx.doi.org/10.1111/j.1600-6143.2010.03242.x

Ford, M.L., and C.P. Larsen. 2009. Translating costimulation blockade to the clinic: lessons learned from three pathways. *Immunol. Rev.* 229:294–306. http://dx.doi.org/10.1111/j.1600-065X.2009.00776.x

Fu, C., and A. Jiang. 2010. Generation of tolerogenic dendritic cells via the E-cadherin/beta-catenin-signaling pathway. *Immunol. Res.* 46:72–78. http://dx.doi.org/10.1007/s12026-009-8126-5

Hawiger, D., K. Inaba, Y. Dorsett, M. Guo, K. Mahnke, M. Rivera, J.V. Ravetch, R.M. Steinman, and M.C. Nussenzweig. 2001. Dendritic cells induce peripheral T cell unresponsiveness under steady state conditions in vivo. *J. Exp. Med.* 194:769–779. http://dx.doi.org/10.1084/jem.194.6.769

Hiramatsu, H., R. Nishikomori, T. Heike, M. Ito, K. Kobayashi, K. Katamura, and T. Nakahata. 2003. Complete reconstitution of human lymphocytes from cord blood CD34+ cells using the NOD/SCID/gammacnull mice model. *Blood*. 102:873–880. http://dx.doi.org/10.1182/blood-2002-09-2755

Hugues, S., L. Fetler, L. Bonifaz, J. Helft, F. Amblard, and S. Amigorena. 2004. Distinct T cell dynamics in lymph nodes during the induction of tolerance and immunity. *Nat. Immunol.* 5:1235–1242. http://dx.doi.org/10.1038/ni1134

Issa, F., J. Hester, R. Goto, S.N. Nadig, T.E. Goodacre, and K. Wood. 2010. Ex vivo-expanded human regulatory T cells prevent the rejection of skin allografts in a humanized mouse model. *Transplantation*. 90:1321–1327. http://dx.doi.org/10.1097/TP.0b013e3181ff8772

Ito, M., H. Hiramatsu, K. Kobayashi, K. Suzue, M. Kawahata, K. Hioki, Y. Ueyama, Y. Koyanagi, K. Sugamura, K. Tsuji, et al. 2002. NOD/SCID/γ(c)(null) mouse: an excellent recipient mouse model for engraftment of human cells. *Blood*. 100:3175–3182. http://dx.doi.org/10.1182/blood-2001-12-0207

Jin, S.M., K.S. Kim, S.Y. Lee, C.H. Gong, S.K. Park, J.E. Yu, S.C. Yeom, T.W. Yoon, J. Ha, C.G. Park, and S.J. Kim. 2010. Enhanced prediction of porcine islet yield and posttransplant outcome using a combination of quantitative histomorphometric parameters and flow cytometry. *Cell Transplant.* 19:299–311. http://dx.doi.org/10.3727/096368909X481638

Kim, H.I., S.Y. Lee, S.M. Jin, K.S. Kim, J.E. Yu, S.C. Yeom, T.W. Yoon, J.H. Kim, J. Ha, C.G. Park, and S.J. Kim. 2009. Parameters for successful pig islet isolation as determined using 68 specific-pathogen-free miniature pigs. *Xenotransplantation*. 16:11–18. http://dx.doi.org/10.1111/j.1399-3089.2008.00504.x

Kim, E.J., B. Choi, H. Moon, Y.J. Lee, Y.K. Jeon, S.H. Park, T.J. Kim, and K.C. Jung. 2011. CD4(+) T cells from MHC II-dependent thymocyte-thymocyte interaction provide efficient help for B cell. *Immunol. Cell Biol.*

Lee, Y.J., Y.K. Jeon, B.H. Kang, D.H. Chung, C.G. Park, H.Y. Shin, K.C. Jung, and S.H. Park. 2010. Generation of $PLZF^+$ $CD4^+$ T cells via MHC class II–dependent thymocyte–thymocyte interaction is a physiological process in humans. *J. Exp. Med.* 207:237–246. http://dx.doi.org/10.1084/jem.20091519

Li, S., Y. Yan, Y. Lin, D.M. Bullens, O. Rutgeerts, J. Goebels, C. Segers, L. Boon, A. Kasran, R. De Vos, et al. 2007. Rapidly induced, T-cell independent xenoantibody production is mediated by marginal zone B cells

and requires help from NK cells. *Blood*. 110:3926–3935. http://dx.doi.org/10.1182/blood-2007-01-065482

Li, W., M.G. Kim, T.S. Gourley, B.P. McCarthy, D.B. Sant'Angelo, and C.H. Chang. 2005. An alternate pathway for CD4 T cell development: thymocyte-expressed MHC class II selects a distinct T cell population. *Immunity*. 23:375–386. http://dx.doi.org/10.1016/j.immuni.2005.09.002

Lou, O., P. Alcaide, F.W. Luscinskas, and W.A. Muller. 2007. CD99 is a key mediator of the transendothelial migration of neutrophils. *J. Immunol*. 178:1136–1143.

Manz, M.G. 2007. Human-hemato-lymphoid-system mice: opportunities and challenges. *Immunity*. 26:537–541. http://dx.doi.org/10.1016/j.immuni.2007.05.001

McGraw, K.J., M.G. Rosenblum, L. Cheung, and D.A. Scheinberg. 1994. Characterization of murine and humanized anti-CD33, gelonin immunotoxins reactive against myeloid leukemias. *Cancer Immunol. Immunother.* 39:367–374. http://dx.doi.org/10.1007/BF01534423

Min, H.S., Y.J. Lee, Y.K. Jeon, E.J. Kim, B.H. Kang, K.C. Jung, C.H. Chang, and S.H. Park. 2011. MHC class II-restricted interaction between thymocytes plays an essential role in the production of innate CD8$^+$ T cells. *J. Immunol.* 186:5749–5757. http://dx.doi.org/10.4049/jimmunol.1002825

Morelli, A.E., and A.W. Thomson. 2007. Tolerogenic dendritic cells and the quest for transplant tolerance. *Nat. Rev. Immunol.* 7:610–621. http://dx.doi.org/10.1038/nri2132

Muller, W.A., and F.W. Luscinskas. 2008. Assays of transendothelial migration in vitro. *Methods Enzymol.* 443:155–176. http://dx.doi.org/10.1016/S0076-6879(08)02009-0

Muller, W.A., and S.A. Weigl. 1992. Monocyte-selective transendothelial migration: dissection of the binding and transmigration phases by an in vitro assay. *J. Exp. Med.* 176:819–828. http://dx.doi.org/10.1084/jem.176.3.819

Muller, W.A., C.M. Ratti, S.L. McDonnell, and Z.A. Cohn. 1989. A human endothelial cell-restricted, externally disposed plasmalemmal protein enriched in intercellular junctions. *J. Exp. Med.* 170:399–414. http://dx.doi.org/10.1084/jem.170.2.399

Reis e Sousa, C. 2006. Dendritic cells in a mature age. *Nat. Rev. Immunol.* 6:476–483. http://dx.doi.org/10.1038/nri1845

Sanchez-Madrid, F., A.M. Krensky, C.F. Ware, E. Robbins, J.L. Strominger, S.J. Burakoff, and T.A. Springer. 1982. Three distinct antigens associated with human T-lymphocyte-mediated cytolysis: LFA-1, LFA-2, and LFA-3. *Proc. Natl. Acad. Sci. USA*. 79:7489–7493. http://dx.doi.org/10.1073/pnas.79.23.7489

Shakhar, G., R.L. Lindquist, D. Skokos, D. Dudziak, J.H. Huang, M.C. Nussenzweig, and M.L. Dustin. 2005. Stable T cell-dendritic cell interactions precede the development of both tolerance and immunity in vivo. *Nat. Immunol.* 6:707–714. http://dx.doi.org/10.1038/ni1210

Shortman, K., and S.H. Naik. 2007. Steady-state and inflammatory dendritic-cell development. *Nat. Rev. Immunol.* 7:19–30. http://dx.doi.org/10.1038/nri1996

Shultz, L.D., F. Ishikawa, and D.L. Greiner. 2007. Humanized mice in translational biomedical research. *Nat. Rev. Immunol.* 7:118–130. http://dx.doi.org/10.1038/nri2017

Smith, C.W., R. Rothlein, B.J. Hughes, M.M. Mariscalco, H.E. Rudloff, F.C. Schmalstieg, and D.C. Anderson. 1988. Recognition of an endothelial determinant for CD 18-dependent human neutrophil adherence and transendothelial migration. *J. Clin. Invest.* 82:1746–1756. http://dx.doi.org/10.1172/JCI113788

Steinman, R.M., and J. Banchereau. 2007. Taking dendritic cells into medicine. *Nature*. 449:419–426. http://dx.doi.org/10.1038/nature06175

Steinman, R.M., D. Hawiger, and M.C. Nussenzweig. 2003. Tolerogenic dendritic cells. *Annu. Rev. Immunol.* 21:685–711. http://dx.doi.org/10.1146/annurev.immunol.21.120601.141040

Strowig, T., C. Gurer, A. Ploss, Y.F. Liu, F. Arrey, J. Sashihara, G. Koo, C.M. Rice, J.W. Young, A. Chadburn, et al. 2009. Priming of protective T cell responses against virus-induced tumors in mice with human immune system components. *J. Exp. Med.* 206:1423–1434. http://dx.doi.org/10.1084/jem.20081720

Subklewe, M., A. Chahroudi, A. Schmaljohn, M.G. Kurilla, N. Bhardwaj, and R.M. Steinman. 1999. Induction of Epstein-Barr virus-specific cytotoxic T-lymphocyte responses using dendritic cells pulsed with EBNA-3A peptides or UV-inactivated, recombinant EBNA-3A vaccinia virus. *Blood*. 94:1372–1381.

Tan, P.H., J.B. Yates, S.A. Xue, C. Chan, W.J. Jordan, J.E. Harper, M.P. Watson, R. Dong, M.A. Ritter, R.I. Lechler, et al. 2005. Creation of tolerogenic human dendritic cells via intracellular CTLA4: a novel strategy with potential in clinical immunosuppression. *Blood*. 106:2936–2943. http://dx.doi.org/10.1182/blood-2005-05-1826

Tarbell, K.V., L. Petit, X. Zuo, P. Toy, X. Luo, A. Mqadmi, H. Yang, M. Suthanthiran, S. Mojsov, and R.M. Steinman. 2007. Dendritic cell–expanded, islet-specific CD4$^+$ CD25$^+$ CD62L$^+$ regulatory T cells restore normoglycemia in diabetic NOD mice. *J. Exp. Med.* 204:191–201. http://dx.doi.org/10.1084/jem.20061631

Tarner, I.H., A.J. Slavin, J. McBride, A. Levicnik, R. Smith, G.P. Nolan, C.H. Contag, and C.G. Fathman. 2003. Treatment of autoimmune disease by adoptive cellular gene therapy. *Ann. N. Y. Acad. Sci.* 998:512–519. http://dx.doi.org/10.1196/annals.1254.067

Tary-Lehmann, M., A. Saxon, and P.V. Lehmann. 1995. The human immune system in hu-PBL-SCID mice. *Immunol. Today*. 16:529–533. http://dx.doi.org/10.1016/0167-5699(95)80046-8

Torres-Aguilar, H., S.R. Aguilar-Ruiz, G. González-Pérez, R. Munguía, S. Bajaña, M.A. Meraz-Ríos, and C. Sánchez-Torres. 2010. Tolerogenic dendritic cells generated with different immunosuppressive cytokines induce antigen-specific anergy and regulatory properties in memory CD4+ T cells. *J. Immunol.* 184:1765–1775. http://dx.doi.org/10.4049/jimmunol.0902133

Traggiai, E., L. Chicha, L. Mazzucchelli, L. Bronz, J.C. Piffaretti, A. Lanzavecchia, and M.G. Manz. 2004. Development of a human adaptive immune system in cord blood cell-transplanted mice. *Science*. 304:104–107. http://dx.doi.org/10.1126/science.1093933

Turnquist, H.R., G. Raimondi, A.F. Zahorchak, R.T. Fischer, Z. Wang, and A.W. Thomson. 2007. Rapamycin-conditioned dendritic cells are poor stimulators of allogeneic CD4$^+$ T cells, but enrich for antigen-specific Foxp3$^+$ T regulatory cells and promote organ transplant tolerance. *J. Immunol.* 178:7018–7031.

van Duivenvoorde, L.M., G.J. van Mierlo, Z.F. Boonman, and R.E. Toes. 2006. Dendritic cells: vehicles for tolerance induction and prevention of autoimmune diseases. *Immunobiology*. 211:627–632. http://dx.doi.org/10.1016/j.imbio.2006.05.014

Wright, S.D., P.E. Rao, W.C. Van Voorhis, L.S. Craigmyle, K. Iida, M.A. Talle, E.F. Westberg, G. Goldstein, and S.C. Silverstein. 1983. Identification of the C3bi receptor of human monocytes and macrophages by using monoclonal antibodies. *Proc. Natl. Acad. Sci. USA*. 80:5695–5703. http://dx.doi.org/10.1073/pnas.80.18.5699

Zahorchak, A.F., L.S. Kean, D. Tokita, H.R. Turnquist, M. Abe, J. Finke, K. Hamby, M.R. Rigby, C.P. Larsen, and A.W. Thomson. 2007. Infusion of stably immature monocyte-derived dendritic cells plus CTLA4Ig modulates alloimmune reactivity in rhesus macaques. *Transplantation*. 84:196–206. http://dx.doi.org/10.1097/01.tp.0000268582.21168.f6